MOLECULAR PROCESSES IN A HIGH TEMPERATURE SHOCK LAYER

Semi-Annual Status Report

May 1,1984-October 31, 1984

NASA Ames Cooperative Agreement NCC 2-308

Steven L. Guberman

Institute for Scientific Research

22 Bonad Road

Winchester, MA 01890

The NASA technical officer for this grant is

Dr. Richard L. Jaffe, Group Leader, Gas Phase Computational Chemistry, STS:230-3, NASA Ames Research Center, Moffett Field, CA 94035

This is the first Semi-Annual status report describing research on molecular processes in a high temperature shock layer.

I. Introduction

Models[1,2] of the shock layer encountered by an Aeroassisted Orbital Transfer Vehicle require as input accurate cross sections and rate constants for the atomic and molecular processes that characterize the shock radiation. From the estimated atomic and molecular densities[2] in the shock layer and the expected residence time of 1 msec[1], it can be expected that electron-ion collision processes will be important in the shock model. Electron capture by molecular ions followed by dissociation, e.g. $O_2^+ + e^- \rightarrow O + O$, can be expected to be of major importance since these processes are known to have high rates (e.g. $10^{-7}cm^3/sec$) at room temperature. However, there have been no experimental measurements of dissociative recombination (DR) at temperatures (>12000K) that are expected to characterize the shock layer. Indeed, even at room temperature, it is often difficult to perform experiments that determine the dependence of the translational energy and quantum yields of the product atoms on the electronic and vibrational state of the reactant molecular ions. This report presents ab initio quantum chemical studies of DR for molecular ions that are likely to be important in the atmospheric shock layer.

II. Summary of Prior Research

A theoretical study of DR involves the determination of potential energy curves[3] for the molecular ion and the dissociative states of the neutral molecule. In order to determine dissociative recombination rates and cross sections one must calculate the electronic probability for electron capture given by Fermi's Golden Rule,

$$\Gamma = 2\pi |\langle P\Psi | H | Q\Psi \rangle|$$

where Ψ is a multiconfiguration wave function and P and Q are Feshbach projection

operators[4] that project onto the terms in Ψ which represent the molecular ion plus a free electron and the terms that represent the autoionizing state respectively . In the usual Feshbach[4] projection operator formalism an eigenvalue equation is derived for $P\Psi$ which is difficult to solve since it contains an energy dependent optical potential. However, I have developed a new technique in which $P\Psi$ can easily be determined by solving the usual configuration interaction (CI) problem. Writing the total wave function as $\Psi = P\Psi + Q\Psi$ we can write the Schroedinger equation in matrix form as

$$\begin{pmatrix} H_{PP} & H_{PQ} \\ H_{QP} & H_{QQ} \end{pmatrix} \begin{pmatrix} P\Psi \\ Q\Psi \end{pmatrix} = E\,1 \begin{pmatrix} P\Psi \\ Q\Psi \end{pmatrix} \tag{1}$$

where $H_{PP} = PHP$, $H_{QP} = QHP$, etc. Multiplying the matrices in (1) leads to:

$$H_{PP}P\Psi + H_{PQ}Q\Psi = EP\Psi \quad \text{and} \tag{2}$$

$$H_{QP}P\Psi + H_{QQ}Q\Psi = EQ\Psi. \tag{3}$$

From (3) we have,

$$Q\Psi = H_{QP}P\Psi/(E - H_{QQ}). \tag{4}$$

Substituting (4) into (2) leads to a matrix optical potential for $P\Psi$,

$$(H_{PP} + H_{PQ}H_{QP}/(E - H_{QQ}))\,P\Psi = EP\Psi. \tag{5}$$

Since E is on both sides of Eq.(5) it is difficult to solve directly for $P\Psi$. However $P\Psi$ can be easily determined by simply diagonalizing the full H matrix in (1) and retaining only the coefficients of the $P\Psi$ configurations. In order to divide by $E - H_{QQ}$ in (4) and to be certain that Q does not mix into the $P\Psi$ that is determined by diagonalizing the H matrix in (1) it is necessary to first solve for the $Q\Psi$ roots by diagonalizing H_{QQ}. The low energy $Q\Psi$ roots are then projected out of the H_{QQ} portion of the H matrix in (1). $P\Psi$ is then determined by diagonalizing

the transformed H matrix. The free electron is represented by a Rydberg orbital with a high principal quantum number. Successive Γ_d's are determined for a series of increasing principal quantum numbers. The widths obtained by this procedure are then extrapolated to the continuum to yield the free electron capture width.

III. Comparison of Ab Initio and Experimental Results

During the past six months these techniques have been tested on the NO molecule where there are experimentally derived[5] interaction matrix elements for the B and L $^2\Pi$ repulsive states of NO. These states are expected to play an important role in the DR of the ground state of NO^+. Using the approach outlined above for calculation of the entrance and exit channel wave functions and the widths, the importance of correlation of the NO 3σ and 4σ orbitals has been investigated in the context of a full valence space CI. These orbitals correspond to the atomic 2s orbitals of N and O at large internuclear separation. Inclusion of valence correlation of the 3σ and 4σ orbitals in the repulsive or autoionizing states increases the B state width and decreases the L state width by about 10% and 40% respectively. In the P space entrance channel the 3σ and 4σ correlation decreases the B and L state widths by 12% and 39% respectively. This inner shell correlation is unimportant for the B state but very important for the L state width. Inner shell correlation has therefore been included in the NO width calculations.

Gallusser and Dressler[5] have reported width matrix elements for the lowest NO $^2\Pi$ Rydberg states. Even though the procedure outlined above uses the high (n=7,8) Rydberg states for extrapolation to the continuum width it is nevertheless instructive to compare our calculated matrix elements for the lowest Rydberg states to the experimentally derived results. For the $B^2\Pi$ repulsive state Hamiltonian matrix element with the $3p\pi$ $C^2\Pi$ Rydberg state the calculated and experimental[5] results are $1229cm^{-1}$ and $1382.6cm^{-1}$ while for the $4p\pi K^2\Pi$ Rydberg state the results

are 714.2cm^{-1} and 803.9cm^{-1} respectively and for the 5pπ Q$^2\Pi$ Rydberg state the results are 484.8cm^{-1} and 594.6cm^{-1} respectively. The difference of only about 11% between theory and experiment for the lower two levels is quite encouraging considering that the matrix elements are quite small and only small valence space CI wave functions have been used. Gallusser and Dressler point out that the Q state matrix element is not as reliable as that for the C state which has the largest matrix element. The experimental Q state matrix element deviates by about 15% from the value predicted from an $n^{*3/2}$ behavior. For the L$^2\Pi$ repulsive state the calculated and experimental matrix elements with the C state are 546.7cm^{-1} and 549.0cm^{-1} respectively while for the K state the results are 320cm^{-1} and -250+50cm^{-1} respectively and for the Q state we have 218.2cm^{-1} and (200cm^{-1}). Gallusser and Dressler[5] have indicated that the Q and K state results are not as reliable as the C state matrix elements with which we obtain excellent agreement.

The NO calculations have been performed with a [3s,2p,1d] basis set for the valence orbitals supplemented by a set of 18 diffuse 2pπ_x Gaussian primitives (centered at the midpoint) for the Rydberg orbitals. The calculations give the contribution of only the l=1 partial wave to the width matrix element. An additional contribution to the Rydberg $^2\Pi$ state widths can be expected from the l=2 partial wave. The l=2 contribution has been calculated by adding to the above basis a set of 12 3d$_{xz}$ Gaussians centered at the midpoint. The l=2 functions increase the B state width by 3.4% and the L state width by 1.7%. Therefore the l=2 wave makes only a minor contribution to the NO $^2\Pi$ widths.

IV Application to O_2^+

Using the above procedure for calculation of the width matrix elements combined with previously calculated potential curves[3] and the quantum defect theory of Giusti[6], cross sections and rate constants have been determined for the DR of O_2^+ leading to O(^{1}S), the upper state of the important atmospheric green line

emission. The calculations include the effect of autoionization, i.e. ejection of the electron after capture and before dissociation occurs. The calculations do not include the effect of indirect recombination through intermediate Rydberg states. Indirect recombination is expected to be important for $O(^1S)$ generation and is the subject of current work.

Fig. 1 shows the calculated rates for particular ion vibrational levels. Clearly, the rate is very sensitive to ion vibrational population. The rates for v=2, 3, and 5 are more than two orders of magnitude greater than the rate for v=0 at low electron temperatures.

Fig. 2 shows the calculated rates as a function of vibrational temperature. As expected from Fig. 1, the rates are sensitive to vibrational temperature at low electron energies but insensitive at high electron energies where Franck-Condon factors become small and autoionization is important. Note that the electron temperature at which the rates become insensitive to vibrational temperature is highly dependent on the shapes of the potential energy curves.

DR calculations over a wide range of temperatures for the remaining dissociative routes of O_2 are currently in progress.

---

1. C. Park, "Radiation Enhancement by Nonequilibrium in Earth's Atmoshphere," AIAA Paper 83-0410, January, 1983.

2. C. Park, "Calculation of Nonequilibrium Radiation in AOTV Flight Regimes," AIAA Paper 84-0306, January, 1984.

3. S. L. Guberman, Potential Energy Curves for Dissociative Recombination, in Physics of Ion-Ion and Electron-Ion Collisions, ed. by F. Brouillard and J. W. McGowan (Plenum, New York, 1983),p.167.

4. H. Feshbach, Ann.Phys.(N.Y.) 5,357(1958).

5. R. Gallusser and K. Dressler, J. Chem. Phys. 76,4311(1982)

6. A. Giusti, J. Phys. B13,3867 (1980).

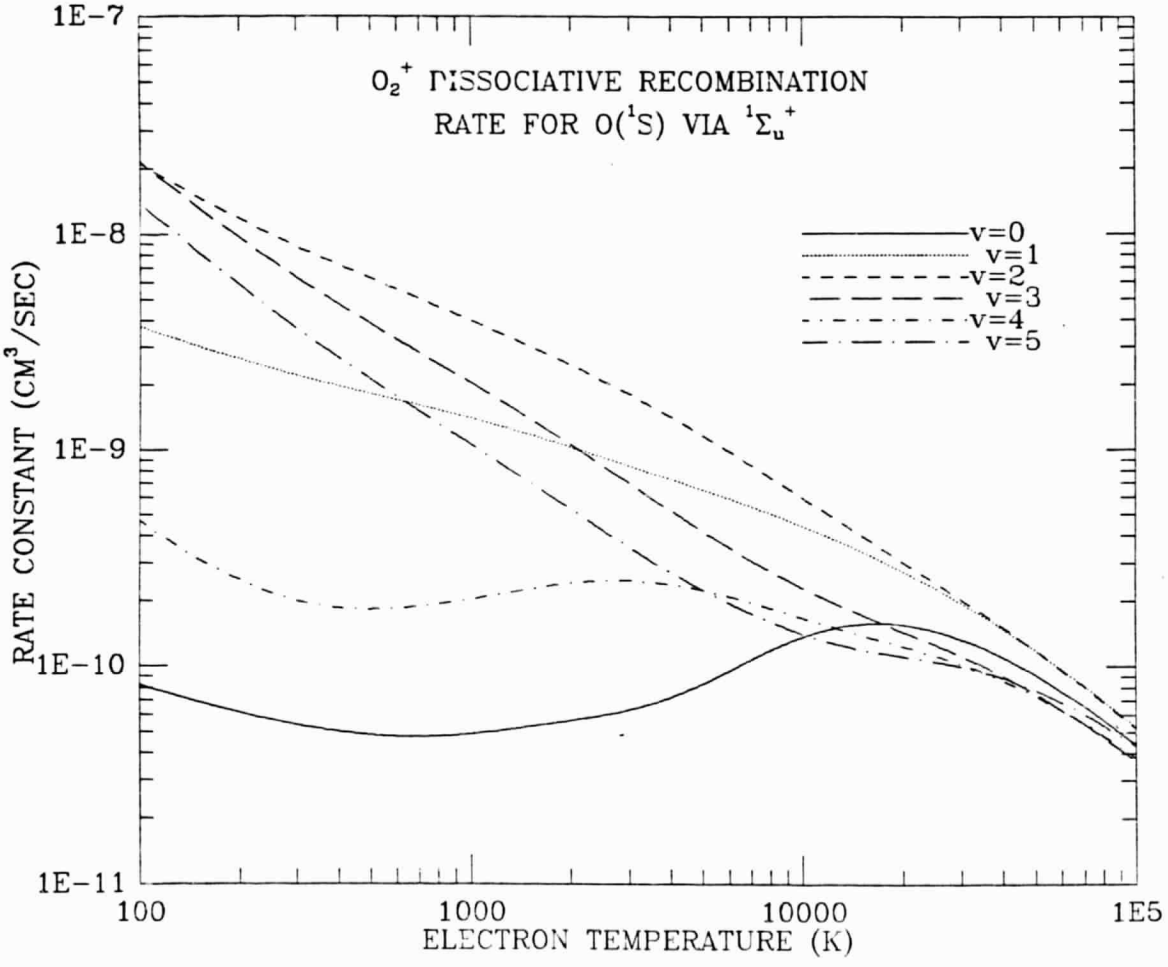
O_2^+ DISSOCIATIVE RECOMBINATION
RATE FOR O(^{1}S) VIA $^1\Sigma_u^+$
v=0
v=1
v=2
v=3
v=4
v=5
RATE CONSTANT (CM^3/SEC)
1E-7
1E-8
1E-9
1E-10
1E-11
100
1000
10000
1E5
ELECTRON TEMPERATURE (K)

Figure 1

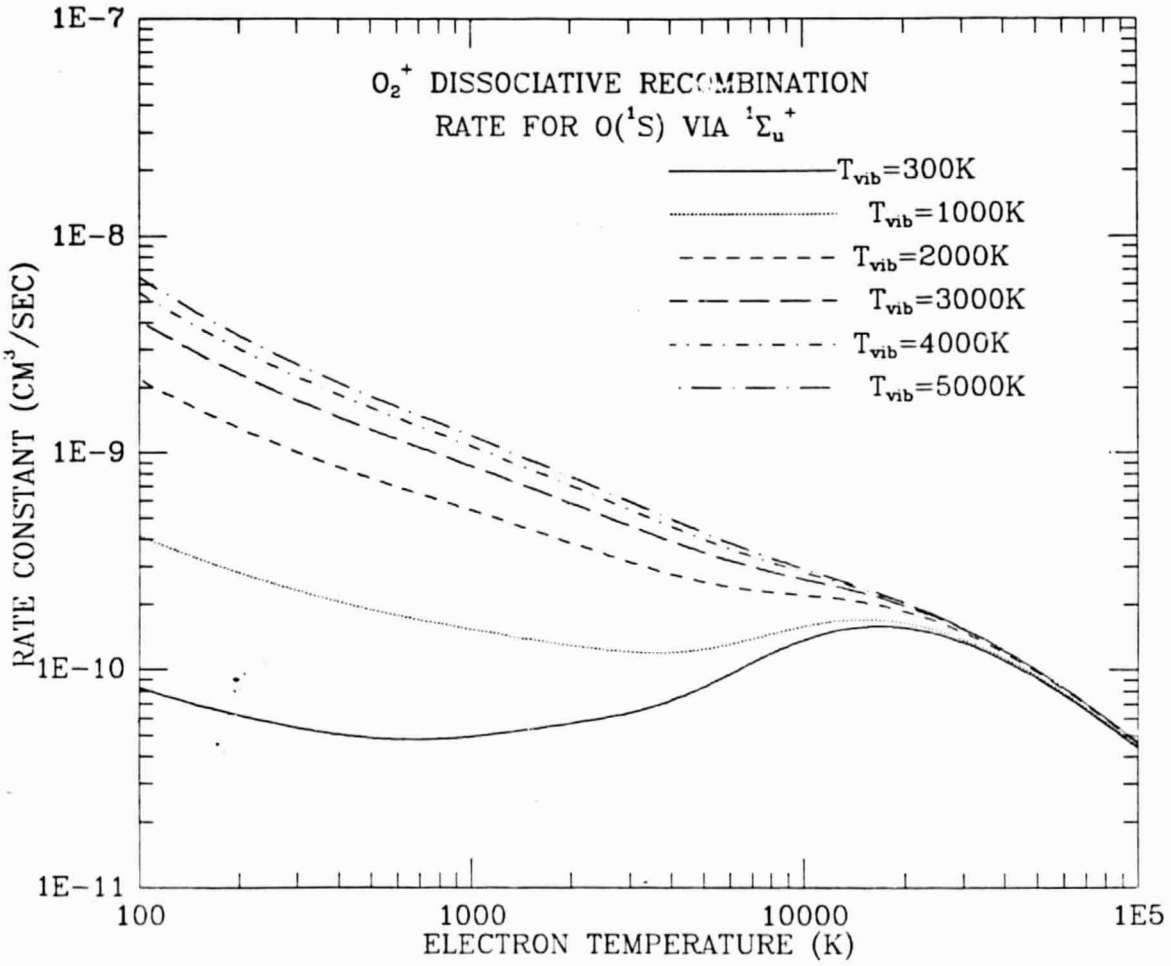
O_2^+ DISSOCIATIVE RECOMBINATION
RATE FOR O(^{1}S) VIA $^1\Sigma_u^+$
T_{vib}=300K
T_{vib}=1000K
T_{vib}=2000K
T_{vib}=3000K
T_{vib}=4000K
T_{vib}=5000K
RATE CONSTANT (CM^3/SEC)
1E-7
1E-8
1E-9
1E-10
1E-11
100
1000
10000
1E5
ELECTRON TEMPERATURE (K)

Figure 2